http://dx.doi.org/10.5935/0103-5053.20130298

J. Braz. Chem. Soc., Vol. 25, No. 3, 453-459, 2014.
Printed in Brazil - ©2014 Sociedade Brasileira de Química
0103 - 5053 $6.00+0.00

Article

Polymer Brush Modified Electrode with Switchable Selectivity Triggered by pH Changes Enhanced by Gold Nanoparticles

Juliane R. Sempionatto, Lucas C. Recco and Valber A. Pedrosa*

Instituto de Biociências, Departamento de Química e Bioquímica, Universidade Estadual Paulista "Júlio de Mesquita Filho" (UNESP), 18618-970 Botucatu-SP, Brazil

Neste trabalho foi desenvolvido um sensor com propriedades inteligentes, baseado em polímeros escova (poli-ácido acrílico) modificado com nanopartículas de ouro. Este novo material demonstrou propriedades comutáveis que podem discriminar diferentes pHs. O eletrodo foi caracterizado por voltametria cíclica (CV), espectroscopia de impedância eletroquímica (EIS) e ressonância plasmônica de superfície localizada (LSPR).

In this work, a sensor was built up with smart material based on polymer brush and gold nanoparticles. The modified electrode functionalized with polyacrylic acid (PAA) tethered to indium tin oxide (ITO) and covered with gold nanoparticle (ITO/PAA/Au) demonstrated switchable interfacial properties discriminating different pHs. The switchable electrochemical and plasmonic process was characterized by cyclic voltammetry (CV), electrochemistry impedance spectroscopy (EIS), and localized surface plasmon resonance (LSPR).

Keywords: polyacrylic acid (PAA), LSPR, polymer brush

Introduction

During the last decades the development of sensors has been the subject of much attention due to an increased demand for sensor and biosensors platforms for environmental monitoring and clinician safety.[1-3] Current efforts have focused on the search for sensors that are economically viable, highly sensitive and selective. Recently, polymer brush thin films activated by external stimuli have attracted considerable interest in the development of sensors for use in chemical and biochemical systems.[4-6] These materials have a high sensitivity to physical or chemical changes occurring in the interface, such as solvent,[7] temperature,[8] ionic strength,[9] light[10] or pH.[11] The pH-induced swelling and collapse of surface-tethered weak polyelectrolyte brushes is of interest not only for the development of responsive surface coatings but also for the pH controlled transport.

Recently, Katz and co-workers studied switchable properties using a modified electrode functionalized with polymer brush composed of poly (4 vinylpyridine) (P4VP).[12] The initial swollen state of the protonated P4VP brush (pH 4.4) was permeable to the anionic $[Fe(CN)_6]^{4-}$ redox species, but the electrochemically produced local pH of 9.1 resulted in the deprotonation of the polymer brush. The produced hydrophobic shrunken state of the polymer brush was impermeable to the anionic redox species, thus fully inhibiting its redox process at the electrode surface. In another paper they reported a pH-responsive mixed polyelectrolyte brush from tethered polyacrylic acid (PAA) and poly(2-vinylpyridine) (P2VP). In pH < 3 the P2VP component was protonated and positively charged, resulting in swollen and hydrophilic domains on the electrode surface, which was permeable for the negatively charged redox species $[Fe(CN_6)^{4-}]$. In the pH range of 4 to 5 the two polymers formed a hydrophobic polyelectrolyte complex, creating a barrier for any charged species, and in pH > 5.5, the carboxylic groups in the PAA became dissociated and negatively charged, creating the negatively charged swollen polymer domains permeable for cationic redox species $[Ru(NH_3)_6^{3+}]$. De Groot *et al.* studied the pH-responsive behavior of the poly(methacrylic acid) (PMAA) brush by scanning electron microscopy (SEM), Fourier transform infrared (FTIR) spectroscopy, and atomic force microscopy (AFM).[13] The swelling behavior of the pH-responsive PMAA brushes was investigated by AFM in aqueous liquid environment with pH values of 4 and 8. AFM images displayed opened polymer chains at pH 4 and closed ones

*e-mail: vpedrosa@ibb.unesp.br

at pH 8, which rationalizes their use as gating platforms. Enhanced higher resistance across the pores was observed in a neutral polymer brush state (lower pH values) and lower resistance when the brush was charged (higher pH values).

Upon pH change, the variation in surface plasmon resonance (SPR) due to the changing interparticle distance could be monitored, showing the potential of the brush/nanoparticle composite to sense changes in pH.[14] Similarly, gold nanoparticles immobilized on P2VP were used for sensing changes in pH by enhanced transmission SPR.[15] Localized surface plasmon resonance (LSPR) have been used to study swelling-shrinking transitions. Several studies have explored highly sensitive nanosensors based on LSPR. The use of LSPR can offer flexibility in their use and high potential for functional nanomaterials. In LSPR, the signal is transduced in transmission mode by measuring the plasmon resonance of metal nanoplasmonic in terms of light absorption. The principle of LSPR was first shown by Gupta and Sannomiya who combined LSPR sensing with electrochemistry to investigate the influence of electrochemical reactions on the LSPR spectrum, using gold nanoparticles immobilized on indium tin oxide (ITO) substrate.[16,17] Tokarev *et al.* reported a stimuli-responsive polymer/noble metal nanoparticle composite thin film based on poly(2-vinylpyridine) brush[18] and by using LSPR in metal nanoparticles to enable the transduction of changes in the solution pH in the near-physiological range into a pronounced optical signal, they related a 50 nm shift to lower wavelength caused by changing the pH from 5.0 to 2.0.

Anchoring polymer chains to a surface can be accomplished by two methods, the "grafting to" approach and the "grafting from" approach. Here, we show a "grafting to" polymer chains assembly by an ends functional polymer chains onto a complementary surface. This method presents the advantage to form a covalent linkage between the polymer chain and the surface. We show the properties resulted from a combination of polymer brush PAA with gold nanoparticles. These brushes into solid-state channels would lead to the creation of robust signal-responsive sensor that can be switched from an "off" state to an "on" state in response to a pH change. The sensor platform demonstrated a pH-sensitive on-off property toward the electroactive probe ferrocene monocarboxylic acid (FMCA) in electrochemical and LSPR responses.

Experimental

Chemicals and reagents

Polyacrylic acid (PAA) (P-3981-AA, MW = 1700 g mol^{-1}, Polymer Source), 3-glycidyloxypropyl-trimethoxysilane (GPS, Sigma-Aldrich), sodium borohydride ($NaBH_4$), trisodium citrate dehydrate, toluene, ferrocene monocarboxylic acid (FMCA) (Sigma-Aldrich), hydrogen tetrachloroaurate(III) ($HAuCl_4 \cdot 3H_2O$). Indium tin oxide (ITO)-coated glass (60 Ω sq^{-1} surface resistivity, Sigma-Aldrich) served as the working electrode, Pt/Ti titanium wire anode ETO78 was employed as a counter electrode, and the reference electrode was a Ag/AgCl (3.0 mol L^{-1}) for electrochemical measurements. Ultrapure water from a Milli-Q (Millipore Inc.) purification system was used in all the experiments.

Modification of electrodes

The ITO electrodes were chemically modified with PAA brushes using the "grafting-to" method according to the following procedure. ITO-coated glass slides were cut into 30 mm × 8 mm strips.[19] They were cleaned with ethanol in an ultrasonic bath for 15 min and dried in the atmosphere. The cleaning step was repeated using 2-butanone as a solvent. The initial cleaning steps were followed by immersing the strips into a cleaning solution composed of NH_4OH, H_2O_2, and H_2O in a ratio of 1:1:1 (v/v/v) for 30 min. Subsequently, the glass strips were rinsed with water and then dried under atmosphere. The freshly cleaned ITO strips were reacted with 0.1% v/v GPS in dry toluene overnight. The silanized ITO was rinsed with several aliquots of toluene. Then 60 μL of a 1% m/m PAA solution in toluene was spin coated to the surface of each ITO glass strip at 3000 rpm and left to react in a vacuum oven at 140 °C overnight. The final cleaning step to remove the unbound polymer consisted of soaking the samples in toluene for 10 min.

Preparation of gold nanoparticles

Finally, citrate ion-stabilized 14 nm diameter gold nanoparticles were adsorbed onto the polymer brush from their aqueous solution. The synthesis of gold nano-particles is described elsewhere.[19] Gold nanoparticles were attached on the PAA polymer brushes from a 1 mmol L^{-1} solution in toluene by incubating the samples overnight. Then the electrode was rinsed by several times with toluene to removed unbound gold nanoparticles.

Equipment and measurement

Electrochemical measurements were performed with an ECO Chemie Autolab Microautolab III/FRA2 with an electrochemical analyzer and the GPES 4.9 (General Purpose Electrochemical System) software package.

Cyclic voltammetry (CV) measurements and Impedance analysis were performed with a three-electrode system in a standard eDAQ (Australia) ET-073 cell, using the polymer brush-modified ITO as working electrode, a Ag/AgCl/KCl 3 mol L^{-1} as a reference electrode, and a Pt/Ti titanium wire anode ETO78 as a counter electrode. The cyclic voltammetry were performed from −0.2 to 0.7 V at scan rates specified in the text and the impedance analysis were recorded while applying a bias potential of 0.3 V and using a 10 mV alternative voltage in the frequency range of 100 kHz-100 mHz. All solutions were buffered (0.1 mol L^{-1} phosphate buffer titrated to the pH values specified in the text with the use of NaOH or HCl) and contained 1.2 mol L^{-1} FMCA as redox probe. Peak currents for each measurement were obtained from a second scan. Before each experiment, a stream of N_2 was passed through the solution for ca. 10 min. The measurements were carried out at ambient temperature (24 ± 2 °C). The pH measurements were performed with a Metrohm 827 pH Lab.

Localized surface plasmon resonance measurements

A series of UV-vis spectra of the ITO/PAA/Au plasmonic platform was obtained by titration with a base from pH 3 to pH 6 using a Biochrom Libra S11 spectrophotometer. The spectroscopic measurements were carried out in PBS (phosphate buffered saline) buffer and a pH range of 3-6 according to the Scheme 1. The specters were taken from 400-600 nm with 1 nm step and speed of 500 nm min^{-1}. A reference of just PBS at specified pH was taken before each scan.

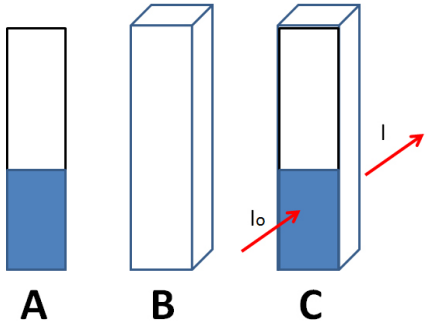

Scheme 1. A: Modified ITO/PAA/Au in a front viewer with an indicative folder; B: conventional glass cuvette and C: cuvette plus ITO, the light is inserted in the back of the sensor.

Results and Discussion

The electrode modification was performed in three steps (Scheme 2): ITO surface silanization (functionalization with epoxy-groups), covalent binding of polyacrylic acid (PAA) linked to the silane thin-film through ester bounds, and finally gold nanoparticle coating.

The experiments were performed in six different pH values: 3.00, 4.00, 4.35, 4.65, 5.00 and 6.00. CVs were taken in a range of scan rate from 20 to 250 mV s^{-1} using FMCA as a redox probe. In the Figure 1, the CV for each pH value is shown, varying the scan rate in the presence of 1.2 mmol L^{-1} of FMCA. The peaks on the cyclic voltammograms were stable and reproducible after many potential cycles, thus confirming that the electrochemical process originates from the surface-confined redox species.

On the inset of each CV (Figure 1) we are able to see a linear correlation between the redox peak currents and the square root of scan rate ($v^{1/2}$); as predicted by the Randles-Sevcik equation for the peak current corresponding to a electrochemical process (i.e., mass transport) dependent on electrode potential and diffusion.[20] This linear correlation indicates a reversible reaction limited by mass transport to the modified electrode surface,[4] the electroactive species have to reach the electrode surface by diffusion for the electron transfer to occur. It means that the electron transfer is controlled by mass transport although the whole process is governed by diffusion. This behavior indicates a good charge transfer between the modified surface and the substrate. Katz and coworkers have found similar behavior using poly(4-vinyl pyridine) functionalized with Os-complex redox units grafting at ITO.[21] They suggested the charge transfer between the conductive support and the redox centers bound to the polymer brush proceeds upon the quasi-diffusional translocation of the polymer chains requiring their flexibility, and the distances between the redox centers are too great for the electron hopping between them.

The kinetic behavior of the modified electrode was analyzed by anodic and cathodic peak current versus potential scan rate and ΔE ($E_p - E^{0'}$; E_p is the peak potential value for the anodic or cathodic branch, and $E^{0'}$ is the formal potential) *versus* log of the potential scan rate. This

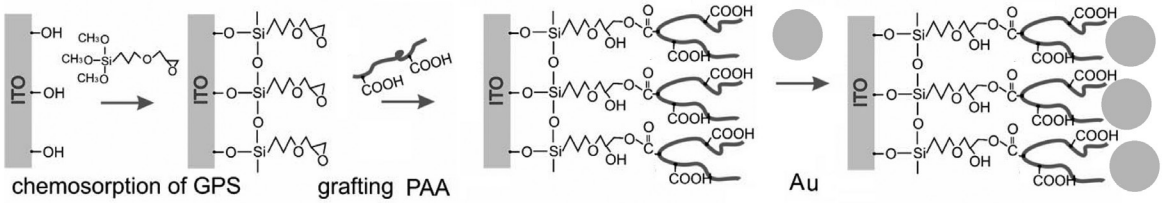

Scheme 2. Modification of substrate: silanization, covalent binding of PAA and gold nanoparticle coating.

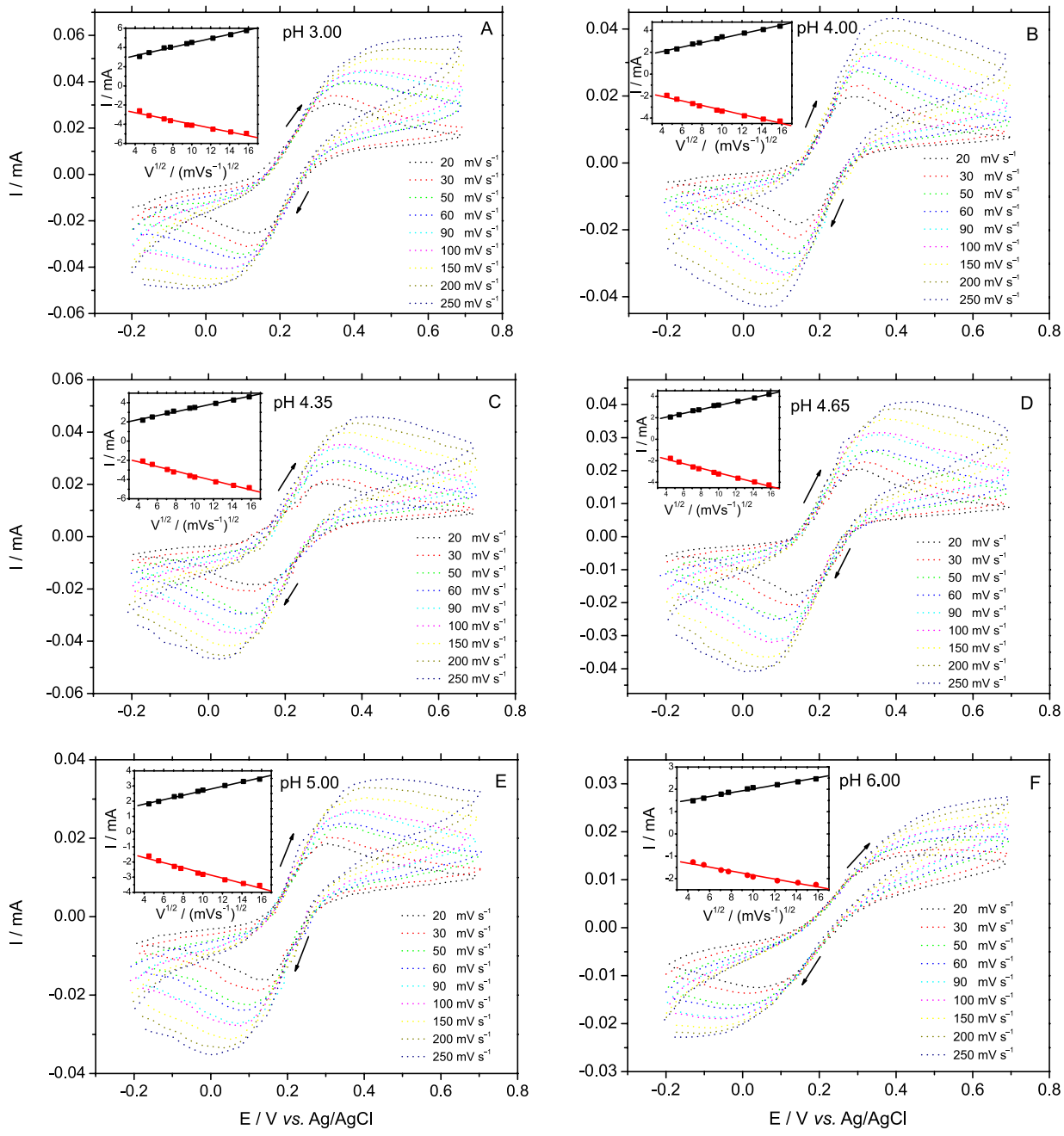

Figure 1. A) CV at pH 3.00; B) CV at pH 4.00; C) CV in pH 4.35; D) CV at pH 4.65; E) CV at pH 5.00; F) CV at pH 6.00.

analysis is used often to better understand the reaction mechanism; a lot of important information can be achieved as the heterogeneous electron-transfer rate constant (k_s). Following the theory, α and k_s can be calculated using equations (1) and (2):

$$\frac{\propto}{1-\propto} = \frac{v_a}{v_c} \quad (1)$$

$$k_s = \frac{nF \propto v_c}{RT} = \frac{(1-\propto) nF v_a}{RT} \quad (2)$$

where F is Faraday's constant, n is the number of electrons, and v_a and v_c are the potential scan rates at intercepts of the straight line fits to anodic and cathodic data, respectively (Figure 2).

Figure 2, obtained from Table 1, shows the Laviron plot with constant ΔE at low scan rates (ΔE is almost independent on the logarithm of scan rate), this fact suggests a fast charge transfer. However, for higher scan rates the peak separations begin to increase, indicating a limitation arising from the charge transfer kinetics. The values of α and k_s were determined to be 0.5 and 3.15 s^{-1},

Table 1. Scan rate ν, anodic (E_a) and cathodic (E_c) peak potentials, formal potential (E^o) and ΔE for Laviron's plot

v / (mV s^{-1})	log (v)	E_a / V	E_c / V	$(E_a+E_c)/2$	E_a-E^o	E_c-E^o
20	1.30	3.06	−2.6	2.83	0.23	−0.23
30	1.47	3.46	−3.09	3.27	0.18	−0.18
50	1.69	3.96	−3.45	3.70	0.25	−0.25
60	1.77	4.04	−3.62	3.83	0.20	−0.20
90	1.95	4.41	−4.07	4.24	0.17	−0.17
100	2.00	4.53	−4.11	4.32	0.21	−0.21
150	2.17	4.98	−4.51	4.74	0.23	−0.23
200	2.30	5.34	−4.8	5.07	0.27	−0.27
250	2.39	5.76	−4.96	5.36	0.40	−0.40

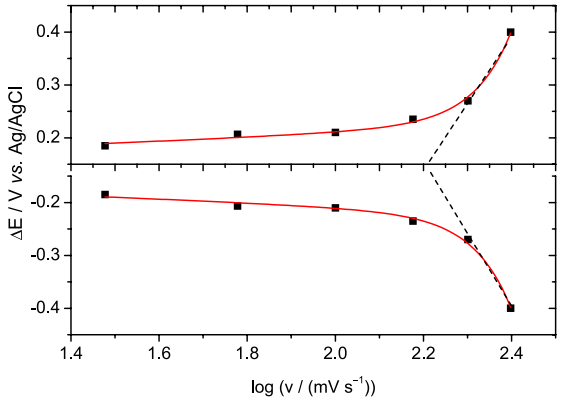

Figure 2. Laviron plot (Ep−E°' *vs.* log potential scan rate) of an ITO/PAA/Au modified electrode in 0.1 mol L^{-1} PBS pH 3.00.

which means that the electronic communication between the redox probe and the electrode surface is fast thereby ensuring that this step is not limiting the interfacial process.

Effect of pH

As we can see in Figure 3, the redox peak intensity, in the scan rate of 50 mV s^{-1}, varies with the pH value, at pH 3.00 we have a maximum current value (0.039 mA) and at pH 6.00 a minimum current value (0.016 mA), this property can be related to a switchable sensor, where in pH 3.00-4.00 it is in an "ON" state, and in pH 6.00 in an "OFF" state.

This behavior can be explained in terms of polymer chain protonation, depending on the solution pH value. The polymer chain of PAA can be protonated or deprotonated, forming domains permeable/impermeable to the redox probe FMCA, which is negatively charged. Our suggestion is in accordance with the work of T. K. Tam *et al.*.[12] They suggest that in pH < 3.5, the PAA is on the shrunken state (OFF state). In the pH range of 4 < pH < 5, the polymer forms hydrophobic polyelectrolyte complex. In the pH values pH > 5.5, the carboxylic groups in the PAA become dissociated with negative charge which is permeable for cationic redox species only. An interesting fact reported in this work, is that at pH < 3.0 the modified electrode shows a maximum of peak current in a scan rate of 50 mV s^{-1} (Figure 3), this fact is not intuitive, since the electrode surface is blocked by shrunken PAA chains, this can be explained due to the gold nanoparticle that enhanced the charge transfer, the same behavior was observed for pH 4.00. In this pH (4 to 5) PAA chains are on a shrunken state forming a hydrophobic polyelectrolyte complex and according to T. K. Tam *et al.*, in this state the collapsed hydrophobic polymer chains create a barrier for the penetration of ionic species regardless of their charges but

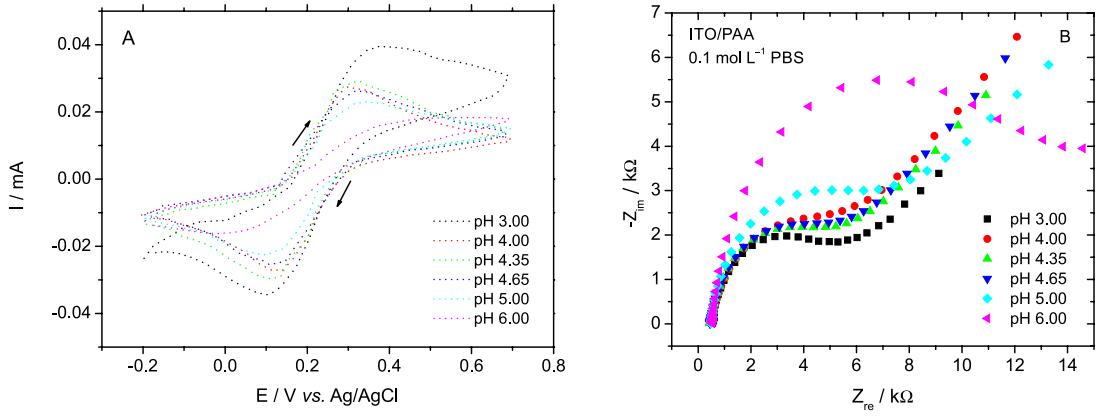

Figure 3. A) CV in a scan rate of 50 mV s^{-1} for the ITO/PAA/Au electrode in pH range from 3.00 to 6.00; B) the respective EIS in same pH range.

we observed a good charge transfer resulting in the redox peak at pH 4.00 to 5.00; we propose this feature due to the presence of the gold nanoparticles.

The switchable properties of the sensor were also studied by electrochemical impedance spectroscopy. Figure 3B shows the heterogeneous electron-transfer resistance, R_{et}, of the FMCA probe calculated by fitting the Nyquist plots; the R_{et} of the redox reactions of FMCA depends on the nature of the reaction and the properties of the electrode/electrolyte interface. The electrolyte solution consisted of 1.2 mmol L^{-1} FMCA with 0.1 mol L^{-1} PBS at the pH from 3.0 to 6.0. The results of the electrochemical impedance study were in agreement with the CV results. Figure 3 demonstrates that the electron transfer is quite facile, when the pH changes from 6.0 to 3.0. This interfacial electron transfer originates from the pH-induced swelling of the polymer brush and results in the formation of ion channels. The switched ON-OFF properties were confirmed by EIS, the resistance value decreases with the increase of solution pH value. In Figure 3B pH 3.00, the semi-circle reaches the minimum value of resistance (5.2 kΩ), while in pH 6.00 reaches the maximum value (13.5 kΩ), confirming the results obtained by CV. The obtained data demonstrate the reversible character of the structural changes in the polymer brush, which swells and shrinks as the pH change. This switch originates from the different states of the polymer brush, in pH 3.0 the polymer is swollen and allows the diffusional translocation of the polymer chains providing the electrochemical accessibility for the pendant redox groups, while in pH 6.0 the polymer is shrunken and the chains movements are "frozen" restricting the electrochemical process. The proposed mechanism is in accordance with the previously reported system based on polymer brushes.[21]

Figure 4 shows the graphs of the redox peak current and potential as function of the pH. The slope of the linear part (E_p/pH, figure 4B) is 63.5 mV *per* pH units over the pH range. This slope is very close to that expected for an electrodic reaction when the e^-/H^+ ratio is equal to one (59.2 (n_p/n_e)) mV *per* pH, where $n_p = n_e$ at 25 °C.[22]

The cyclic voltammograms demonstrate that the oxidation and reduction peak potentials as the redox peak current values have a dependence with the pH value (Figure 4A-B), the anodic/cathodic peak current increases with the increase of scan rate as the potential peak values dislocates to positive/negative potentials.

LSPR measurements were performed to confirm the attachment of the gold nanoparticles on the polymer brush endings. In Figure 5, we are able to see the shift caused by the different solution pHs.

The measurements confirmed that the film was sensitive to pH changes in terms of different interaction of charges with gold nanoparticles. The response shows a blue shift (from 530 to 524 nm) after increasing pH from 3.0 to 4.65 and a red shift (524 to 526 nm) when the pH increased from pH 4.65 to 6.00, for the ITO/PAA/Au electrode. This behavior could be due to the appearance of negative charge, because in the pH range of 4 < pH < 5 the polymer forms a hydrophobic polyelectrolyte complex, generating a blue shift, and at higher pH values and pH > 5.5, the carboxylic groups in the PAA become dissociated and negatively charged, in this case a red shift occurs. Changes in absorption spectra were reproducible, indicating that the PAA brushes take a reversible stretching motion depending on the pH change, whereas gold nanoparticles are tethered firmly on the solid substrates. The spectral shifts have shown a reversible behavior as confirmed by repeating the pH change for couple of times, which implies that the system is stable and reversible. These data are consistent with the results obtained from CV experiments and demonstrate that the gold nanoparticles are successfully immobilized on the brush-modified electrode. In Figure 5B we are able to see the titration curve of the ITO/PAA/Au electrode, with the pH range varying from 3.00 to 6.00. In a pH range from 3.50 to 4.50 there is a linear behavior, the linear fit of this range indicates an almost 6 nm shift

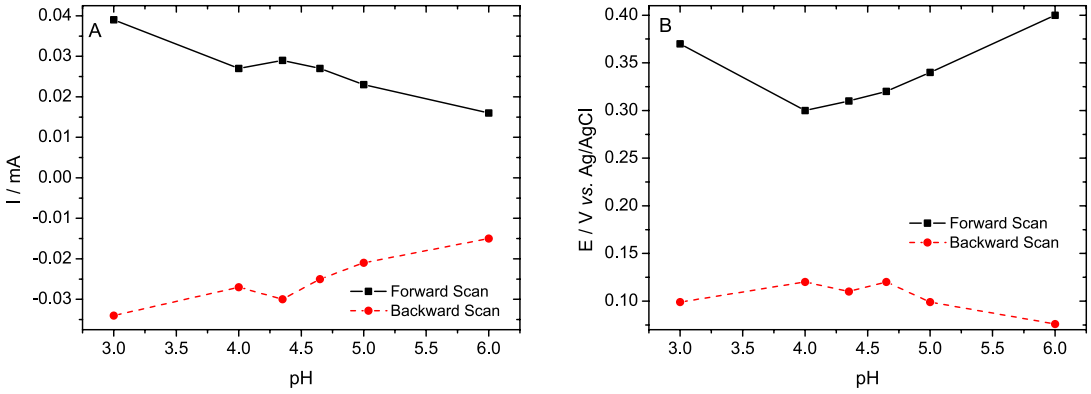

Figure 4. ITO/PAA/Au electrode. A) Current value variation *vs* pH, scan rate 50 mV s^{-1}; B) peak potential variation *vs.* pH, scan rate 50 mV s^{-1}.

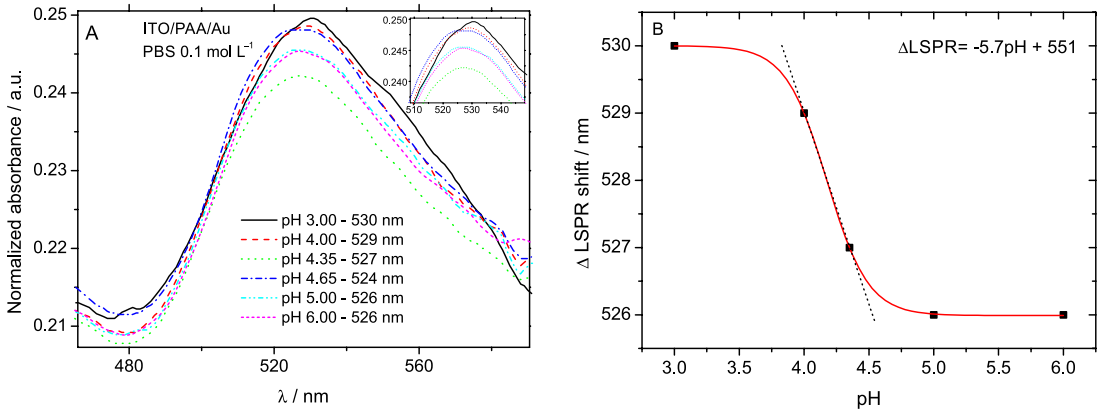

Figure 5. A) LSPR in a pH range from 3.00 to 6.00 for ITO/PAA/Au electrode; B) titration curve pH 3.00 to 6.00.

for each pH unit change. This pH-sensing range suggests potential application for pH determination.

Conclusion

The switchable properties of polyacrylic acid (PAA) brush modified with gold nanoparticles were evaluated by different methods. The results obtained were in accordance with previously works; additionally we were able to demonstrate an improvement in the charge transfer by using gold nanoparticles. The enhancement of the system properties were due to the gold nanoparticles immobilized on the brush-modified electrode, the immobilization was confirmed by LSPR measurements. With this report, we expect to contribute knowledge about the polymer brush system, which is certainly an outstanding candidate for lots of sensor platforms.

Acknowledgement

The authors thank FAPESP (2010/07478-5, 2013/12623-2), CAPES and CNPq, Brazil, for the grants and the financial support to this work.

References

1. Szunerits, S.; Boukherroub, R.; *Chem. Commun*. **2012**, *48*, 8999.
2. Lee, H. S.; Eckmann, D. M.; Lee, D.; Hickok, N. J.; Composto, R. J.; *Langmuir* **2011**, *27,* 12458.
3. Yao, H.; Hu, N.; *J. Phys. Chem. B* **2010**, *114*, 3380.
4. Antonio, T. R. T. A.; Basso, C. R.; Cabral, M. F.; Pedrosa, V. A.; *Int. J. Electrochem. Sci.* **2013**, *8*, 4150.
5. Tam, T. K.; Zhou, J.; Pita, M.; Ornatska, M.; Minko, S.; Katz, E.; *J. Am. Chem. Soc*. **2008**, *130*, 10880.
6. Yao, H.; Hu, N.; *J. Phys. Chem. B* **2010**, *114*, 9926.
7. Ahn, S. J.; Kaholek, M.; Lee, W. K.; LaMattina, B.; LaBean, T. H.; Zauscher, S.; *Adv. Mater*. **2004**, *16*, 2141**.**
8. Sun, T. L.; Wang, G. J.; Feng, L.; Liu, B. Q.; Ma, Y. M.; Jiang, L.; Zhu, D.; *Angew. Chem., Int. Ed.* **2004**, *43*, 357.
9. Motornov, M.; Sheparovych, R.; Katz, E.; Minko, S.; *ACS Nano* **2008**, *2*, 41.
10. Wittemann, A.; Drechsler, M.; Talmon, Y.; Ballauff, M.; *J. Am. Chem. Soc*. **2005**, *127*, 9688.
11. Ionov, L.; Houbenov, N.; Sidorenko, A.; Stamm, M.; Minko, S.; *Adv. Funct. Mater*. **2006**, *16*, 1153.
12. Tam, T. K.; Zhou, J.; Pita, M.; Ornatska, M.; Minko, S.; Katz, E.; *J. Am. Chem. Soc.* **2008,** *13*, 010880.
13. Groot, W. G.; Santonicola, G. M.; Sugihara, K.; Zambelli, T.; Reimhult, E.; Vörös, J.; Vancso, G. J.; ACS Appl. Mater. Interfaces **2013**, *5*, 1400.
14. Basso, C. R.; Santos, B. L.; Pedrosa, V. A.; *Electroanalysis* **2013**, *25*, 1818.
15. Tokareva, I.; Minko, S.; Fendler, J. H.; Hutter, E.; *J. Am. Chem. Soc.* **2004**, *126*, 15950.
16. Gupta, S.; Agrawal, M.; Uhlmann, P.; Simon, F.; Oertel, U.; Stamm, M.; *Macromolecules* **2008**, *41*, 8152.
17. Sannomiya, T.; Dermutz, H.; Hafner, C.; Vörös, J.; Dahlin, A. B.; *Langmuir* **2010**, *26*, 7619.
18. Tokarev, I.; Motornov, M.; Minko, S.; *J. Mater. Chem*. **2009**, *19*, 6932.
19. Roiter, Y.; Minko, I.; Nykypanchuk, D.; Tokarev, I.; Minko, S.; *Nanoscale* **2012**, *4*, 284.
20. Southampton Electrochemistry Group. In *Instrumental Methods in Electrochemistry,* vol. 1, 1st ed.; Ellis Horwood Ltd: Chichester, UK, 1990.
21. Tam, T. K.; Ornatska, M.; Pita, M.; Minko, S.; Katz, E.; J. Phys. Chem. C **2008**, *11*, 28438.
22. Tam, T. K.; Pita, M.; Trotsenko, O.; Motornov, M.; Tokarev, I.; Halámek, J.; Minko, S.; Katz, E.; *Langmuir* **2010**, *26*, 4506.

Submitted: October 15, 2013
Published online: December 13, 2013

FAPESP has sponsored the publication of this article.